Association of heat shock protein 8 with atopic march in a murine experimental model

Kyu-Tae Jeong [1], **Ji-Hye Do** [1], **Sung-Hee Lee** [1], **Jeom-Kyu Lee** [1], **Woo-Sung Chang** [Corresp. 1]

[1] Division of Allergy and Respiratory Disease Research, Department of Chronic Disease Convergence Research, Korea National Institute of Health, Korea Disease Control and Prevention Agency, Cheongju, Osong-eup, Heungdeok-gu, Korea

Corresponding Author: Woo-Sung Chang
Email address: cws99@korea.kr

Background. Atopic march (AM), a unique characteristic of allergic diseases, refers to the sequential progression of atopic dermatitis (AD) in infants to allergic asthma and allergic rhinitis in children and young adults, respectively. Although several studies have reported on AM, the establishment of an AM murine model to expand our understanding of the underlying mechanism and to identify the potential biomarkers is yet to be achieved. In this study, an improved murine model was established by applying a method to minimize skin irritation in inducing AD, and it was used to perform integrated analyses for candidate biomarker discovery.

Methods. We applied *Dermatophagoides pteronyssinus* (Dp) extract with 2,4-dinitrochlorobenzene on female BALB/c mice ears twice a week for 5 consecutive weeks, followed by Dp sensitization and intranasal challenges for 4 weeks to develop conditions mimicking AM.

Results. Exacerbated airway inflammation and allergic responses observed in the AM-induced group suggested successful AM development in our model. Two-dimensional gel electrophoresis (2-DE) and mass spectrometry analysis identified 753 candidate proteins from 124 2-DE spots differentially expressed among the experimental groups. Functional analyses, such as Gene Ontology (GO) annotation and protein–protein interaction (PPI) analysis were conducted to investigate the relationship among the candidate proteins. Seventy-two GO terms were significant between the two groups; heat shock protein 8 (Hspa8) was found to be included in six of the top 10 GO terms. Hspa8 scored high on the PPI parameters as well.

Conclusion. We established an improved murine model for AM and proposed Hspa8 as a candidate biomarker for AM.

Association of heat shock protein 8 with atopic march in a murine experimental model

Kyu-Tae Jeong, Ji-Hye Do, Sung-Hee Lee, Jeom Kyu Lee, and Woo-Sung Chang*

Division of Allergy and Respiratory Disease Research, Department of Chronic Disease Convergence Research, Korea National Institute of Health, Korea Disease Control and Prevention Agency, Cheongju, Korea

Corresponding Author:
Woo-Sung Chang, Ph.D.
Division of Allergy and Respiratory Disease Research, Department of Chronic Disease Convergence Research, Korea National Institute of Health, Korea Disease Control and Prevention Agency, Cheongju, Korea
Email address: cws99@korea.kr

Abstract

Background. Atopic march (AM), a unique characteristic of allergic diseases, refers to the sequential progression of atopic dermatitis (AD) in infants to allergic asthma and allergic rhinitis in children and young adults, respectively. Although several studies have reported on AM, the establishment of an AM murine model to expand our understanding of the underlying mechanism and to identify the potential biomarkers is yet to be achieved. In this study, an improved murine model was established by applying a method to minimize skin irritation in inducing AD, and it was used to perform integrated analyses for candidate biomarker discovery.

Methods. We applied *Dermatophagoides pteronyssinus* (Dp) extract with 2,4-dinitrochlorobenzene on female BALB/c mice ears twice a week for 5 consecutive weeks, followed by Dp sensitization and intranasal challenges for 4 weeks to develop conditions mimicking AM.

Results. Exacerbated airway inflammation and allergic responses observed in the AM-induced group suggested successful AM development in our model. Two-dimensional gel electrophoresis (2-DE) and mass spectrometry analysis identified 753 candidate proteins from 124 2-DE spots differentially expressed among the experimental groups. Functional analyses, such as Gene Ontology (GO) annotation and protein–protein interaction (PPI) analysis were conducted to investigate the relationship among the candidate proteins. Seventy-two GO terms were significant between the two groups; heat shock protein 8 (Hspa8) was found to be included in six of the top 10 GO terms. Hspa8 scored high on the PPI parameters as well.

Conclusion. We established an improved murine model for AM and proposed Hspa8 as a candidate biomarker for AM.

Introduction

Over the years, the prevalence and burden of allergic diseases, such as asthma, allergic rhinitis, and atopic dermatitis (AD), have been increasing worldwide (Eder et al. 2006; Odhiambo et al. 2009; Platts-Mills 2015). Atopic march (AM), a distinctive feature underlying allergic disease, is characterized by the sequential progression of allergic diseases, such as AD in infants, followed by allergic asthma and allergic rhinitis in children and young adults, respectively (Aw et al. 2020; Cohn et al. 2004; del Giudice et al. 2006). The concept of AM primarily revolves around the fact that the presence of one allergic disease leads to an increased risk for others, suggesting the presence of a causal relationship among the allergic diseases (Bantz et al. 2014; Hill & Spergel 2018). Recently, our understanding of AM has been expanded by several cohort studies and evidence obtained from experimental murine models. Previous studies have revealed the presence of asthma, allergic rhinitis, and one or more atopic comorbidities in infants with greater AD severity (Gustafsson et al. 2000; Schneider et al. 2016). A prospective birth cohort study revealed that children with a combination of AM and allergic sensitization in early life are likely to have an increased risk of asthma and food allergies at the age of 3 years (Tran et al. 2018). In terms of AM pathogenesis, multiple data from animal models support the hypothesis that allergen exposure through inflamed skin is the primary route for systemic type 2 inflammation causing AM (Hill & Spergel 2018; Hogan et al. 2012).

The concept of AM is considered important and helpful in the early recognition of subsequent diseases and identification of infants at high risk of allergic progression (Busse 2018). Despite a

variety of studies on the mechanism or interventions for AM, diverse approaches are warranted to expand the understanding of the relationships among allergic diseases and develop strategies for preventive interventions. In this regard, a murine model for AM is required to provide insight into the mechanism of AM and find the potential biomarkers that could be utilized in the strategies for AM.

In this study, we aimed to establish a murine experimental model for AM by sequentially provoking asthma after the induction of AD by minimizing skin irritation caused by hair removal. We then applied two-dimensional gel electrophoresis (2-DE) analysis and mass spectrometry (MS) to identify the differentially expressed proteins in the bronchoalveolar lavage fluid (BALF) between control and AM-induced mice. Functional and network analyses were conducted to find candidate biomarkers in AM by investigating the significance of the identified proteins and their interaction.

Materials & Methods

Animals

Female BALB/c mice (5 weeks old) were purchased from Orient Bio (Seongnam, Korea). The mice were housed in the animal research center of Korea Disease Control and Prevention Agency at a controlled ambient temperature of 22 °C with 50 ± 20% relative humidity under a 12 h light-dark cycle (lights on at 7:00 AM). A total of 60 mice, 20 in 3 independent sets, were used for this study. We randomly divided the mice into each experimental group. Animal care and experimental protocols were approved by the Institutional Animal Care and Use Committee of the Korea Centers for Disease Control and Prevention (KCDC-031-16-2A, KCDC-033-17-2A, KCDC-121-17-2A, KCDC-019-19-2A, KCDC-034-20-2A).

Murine model for AM

The extract of *Dermatophagoides pteronyssinus* (Dp), a major species of house dust mite, purchased from Prolagen (PEA-DERP010, Yonsei University College of Medicine, Seoul, Korea), was re-suspended in phosphate-buffered saline (PBS). To induce AD, a previously published protocol (Choi & Kim 2014; Kim et al. 2013) with minor modifications was used. Once a week, 1% 2,4-dinitrochlorobenzene (DNCB) (20 μL of a 4:1 mixture of acetone/olive oil) was applied to the ear skin, and this was continued for 5 weeks (days −7, −2, 5, 12, 19). From the

second application of DNCB, 75 μg of Dp (in 20μL of PBS) or PBS was topically applied 2 days after the DNCB application; this was continued for 4 weeks (days 0, 7, 14, 21). Barrier disruption was achieved by applying 20 μL of 4% sodium dodecyl sulfate to the ear skin 4 h before the application of Dp or PBS. The condition of the skin lesion was measured using digital photographs taken after anesthesia once a week, and plasma was obtained to measure the level of immunoglobulin E (IgE) on days 8 and 22. For the subsequent development of asthma, 4 μg of Dp (in 200μL of PBS) or PBS was intraperitoneally administrated on days 25 and 39, followed by intranasal challenges with 8 μg of Dp (in 40μL PBS) or PBS for 4 consecutive days from day 46 to 49 (Fig. 1). Twenty-four hours after the last challenge, mice were anesthetized and measured airway hyperresponsiveness (AHR) as described below. Immediately following the measurement of AHR, mice were euthanized with an overdose of sodium pentobarbital to obtain plasma, BALF, and lung tissues for further analysis. PBS-treated mice both in the step of AD induction and asthma development served as the normal control (NC) group. For the AD-induced group, the mice were treated with Dp in the step of AD induction and PBS in the step of asthma development. Mice treated with PBS in the AD step and Dp during asthma development served as the asthma (AS)-induced group. Dp-treated mice in both steps served as the AM-induced group. We established the humane endpoints that the mice were euthanized under deep anesthesia if any of signs such as weight loss, lethargy, or dyspnea were seen during all the experiments; however, these were not needed in this study.

Measurement of AHR

AHR was measured using the flexi-Vent system (flexiVent Fx1; SCIREQ, Montreal, Quebec, Canada) according to the manufacturer's protocol. Briefly, mice were anesthetized with 50 mg/kg sodium pentobarbital, and tracheostomy was performed. Mice were then intubated with a blunt needle and connected to a small-animal ventilator with a computer-controlled piston. PBS and an increasing doses of methacholine (12.5, 25, and 50 mg/mL; Sigma-Aldrich, St. Louis, MO, USA) were inhaled, and the parameters of AHR, such as airway resistance and compliance, were measured.

Enzyme-linked immunosorbent assay

Blood samples, collected and stored for 2 h at room temperature, were subjected to centrifugation (4,000 rpm for 10 min), and the supernatants obtained were harvested and stored at −70 °C. Total IgE was measured using a sandwich enzyme-linked immunosorbent assay (ELISA) kit (Biolegend, San Diego, CA, USA) according to the manufacturer's protocol. BALF from each group was collected and centrifuged immediately (13,000 rpm, 5 min). The supernatants obtained were harvested and stored at −70 °C. The levels of interleukin (IL)-4, IL-5, IL-13, and interferon (IFN)-γ in the BALF samples were measured using sandwich ELISA kit (R&D Systems, Inc., Minneapolis, MN, USA), according to the manufacturer's protocol.

Quantification of Dp-specific IgE

To detect Dp-specific IgE, the antigen-capture ELISA method was used with minor modifications. Briefly, 96-well plates were coated with 10 μg of Dp in 100 μL of coating buffer. After overnight incubation at 4 °C, the plates were blocked with 200 μL/well of assay diluent. Thereafter, 100-μL aliquots of undiluted plasma were added to each well and incubated at room temperature for 1 h. Again, 100 μL of biotin-anti-mouse IgE (Biolegend) was added to each well and incubated for 2 h. After incubation with avidin horse radish peroxidase (BioLegend) for 30 min, 3,3′,5,5′-tetramethylbenzidine substrate solution (100 μL, Invitrogen) was added to each well and incubated in the dark for 20 min. The reaction was stopped with 2 N sulfuric acid. Optical densities were read at 450 nm with a reference wavelength of 570 nm using the SpectraMax i3x microplate reader (Molecular Devices, San Jose, CA, USA).

Analysis of immune cells in the BALF

Red blood cells (RBCs) in the precipitated cells obtained from the BALF samples as described above were removed using RBC Lysis buffer (Sigma-Aldrich). The total cells were counted using Nucleo Counter (ChemoMetec, Allerød, Denmark) and stained with Diff-Quick solution (Sysmex Corporation, Hyogo, Japan). The number of eosinophils, macrophages, monocytes, lymphocytes, and neutrophils was determined by counting at least 200 cells in each of four different locations.

Histological analysis of lung tissue

Lobes of the left lung were removed, washed in PBS, and fixed in 4% buffered formalin solution for 3 days. Fixed lung tissues were dehydrated, clarified, and embedded in paraffin. Lung sectioning, subsequent staining with hematoxylin and eosin (H&E, Sigma-Aldrich) and slide scanning were conducted to evaluate general morphology under light microscopy (AXIO Imager 2; Carl Zeiss, Oberkochen, Germany).

Identification of proteins in the BALF using 2-DE

Proteins in the BALF were precipitated using acetone. After quantification, the precipitated proteins were separated by 2-DE. The gel was scanned using the ChemiDoc gel imaging system (Bio-Rad Laboratories, Inc., Hercules, CA, USA) to detect the density and distribution of the protein spots. Proteins in excised gel spots were identified with technical support from Proteinworks (Daejeon, Korea) by liquid chromatography-MS/MS (LC-MS/MS) analysis and MASCOT search.

Functional annotation

The National Center for Biotechnology Information Resference Sequence or Genebank IDs of 2-DE spot proteins were converted to a UniProt Knowledgebase (UniProt KB) IDs using the Database for Annotation, Visualization and Integrated Discovery (DAVID) gene ID conversion tool (Huang da et al. 2008). The proteins contained actin or albumin and duplicated proteins were eliminated. Next, the functions of candidate proteins were analyzed using DAVID version 6.8 (http://david.abcc.ncifcrf.gov/) (Huang da et al. 2009), which is a web-based functional annotation tool for investigators to analyze the biological roles of genes and is applied to perform Gene Ontology (GO) analysis. For significant GO terms, $p < 0.05$ was considered as the cut-off criterion.

Protein–protein interaction (PPI) network

A PPI network of proteins was constructed using the STRING database version 11 (http://string-db.org/) (Szklarczyk et al. 2019), and the protein interaction relationship network was visualized using Cytoscape software (Shannon et al. 2003). The default parameter for selecting a significant interaction pair from the STRING database was 0.4. Then, according to the interaction scores of the PPI network, the Cytoscape plug-in NetworkAnalyzer was used for further analysis. The

topological properties of the PPI network and node degree were calculated to search for hub genes from the PPI network. Several different centralities, such as degree, betweenness, closeness, eigenvector, and stress distributions were provided for more screening, but the main connected component of the PPI network was layout by degree values. Degree centrality counts the number of edges at each node and betweenness centrality determines which nodes are important in the flow of the network.

Statistical analysis

The values are presented as means ± standard error of the mean. Statistical comparisons between groups were conducted using the Student's *t*-test with $p < 0.05$ as the cut-off criterion for statistical significance.

Results

The induction of AD-like skin lesions by repeated topical application of Dp

As the first step for the establishment of the AM model, Dp and DNCB were topically applied alternatively once a week for 4 weeks to induce AD. We applied them on mouse ears to minimize the skin irritation caused by hair removal. AD-like lesions consisting of erythema and excoriation and damage to the epidermal layer were developed in the AD-induced group (Fig. 2A). The total IgE level in plasma was significantly higher in the AD-induced group than in the NC group (Fig. 2B), indicating the induction of the allergic response. These results suggested that AD was well- developed by the repeated topical application of Dp with DNCB only on the ears.

Exacerbation of AHR and airway inflammation in the AM-induced group

After the successful induction of AD, asthma was sequentially provoked by Dp sensitization and intranasal challenges to develop conditions that mimic AM. We performed Dp challenges daily for the last 4 days, followed by measuring the main parameters that indicate the development of asthma. Airway resistance, as a parameter for AHR, was significantly higher in the AM-induced group than that in the AD-only or asthma-only induced groups (Fig. 3A). The number of eosinophils in BALF was higher in the AM-induced group than in the asthma-only induced and NC groups. Cell infiltration observed by H&E staining in lung tissue was also worse in the AM-

induced group than in the other groups (Fig. 3B and 3C). These results demonstrate that airway inflammation was exacerbated in the AM-induced group that AD and asthma were sequentially induced.

Highly elevated IgEs and cytokines in the AM-induced group

To investigate whether allergic responses were aggravated under the AM-mimicking conditions, we measured the level of IgEs, T helper type 2 (Th2), and inflammatory cytokines in the BALF. The levels of total and Dp-specific IgE were significantly higher in the AM-induced group than in the AD or asthma-only induced groups (Fig. 4A and 4B). Likewise, the Th2 cytokine levels, including those of IL-4, IL-5, and IL-13, were also higher in the BALF obtained from the AM-induced group than that from the other groups (Fig. 4C–4F). However, the level of IFN-γ, a key cytokine for the Th1 response, was significantly lower in the AM-induced group than in the other groups. Thus, the aggravation of the allergic reactions was mediated by Th2 responses under our AM-mimicking conditions. These findings and the exacerbated airway inflammation described above indicate the successful establishment of the murine model for AM.

Identification of hub proteins and pathways by functional analyses

To identify candidate biomarkers for AM, we next investigated the proteins that were differentially expressed among the groups in our model. Through the 2-DE analysis of 28 sets of 92 gels that were loaded with BALF samples from each experimental group, 124 differentially expressed spots (> 1.5 fold) were detected. LC-MS/MS analysis and MASCOT search were performed to identify the candidate proteins that each spot represented. A total of 753 candidate proteins, including 406 proteins that were differentially expressed in the AM-induced group compared with the NC, were identified. We then analyzed functional annotation and PPI to determine the biological relationship among the identified proteins. Of the 232 GO terms significantly enriched by GO annotation ($p < 0.05$), 72 GO terms showed a significant enrichment between the AM-induced and the NC groups. As shown in Table 1, six of the Top 10 GO enriched terms were classified into the cellular component group, and we found that Hspa8 was included in all six terms. Furthermore, PPI analysis using the STRING database and Cytoscape tool also showed Hspa8 as one of the highest scoring proteins based on the PPI

parameters, such as degree, betweenness centrality, and closeness centrality (Table 2), and Hspa8 was represented as a hub node in the network of the differentially expressed protein (Fig. 5).

Discussion

In this study, we established a murine experimental model for AM by applying a method for the minimization of skin irritation during AD development. AD-like lesions, such as erythema and excoriation, with elevated total IgE in plasma were observed by the repeated topical application of Dp and DNCB for 8 consecutive weeks. After the subsequent development of asthma, airway inflammation and allergic responses were aggravated in the AM-induced group, indicating that AM-mimicking conditions were well triggered in our model. Under the concept of AM, the AD development and allergen sensitization in infants predispose them to subsequent development of other allergic diseases, including asthma (Han et al. 2017). Murine experimental models facilitate the understanding of the underlying mechanisms of AM development and aid in the design of various therapeutic approaches for the prevention and treatment of allergic diseases, despite the debates citing inappropriateness of the approach owing to poor reproducibility and limited translation in humans (Justice & Dhillon 2016). Lee et al. suggested that the repeated application of topical acidic cream in a murine model of AM with oxazolone-induced AD inhibits respiratory allergic inflammation and AD-like skin lesions, suggesting acidification of the stratum corneum (SC) to be a novel intervention method for AM (Lee et al. 2014). In another study involving an Nc/Nga mouse-based AM model, they reported the importance of preventing a neutral environment on the SC to alleviate AM-related symptoms (Lee et al. 2015). Probiotic treatment in a murine model for AM increased the level of regulatory T cells, which could suppress the cytokine-mediated responses associated with the progression of AM (Kim et al. 2014). Although these murine experimental models were used in various studies on AM, they had several limitations associated with the induction of AD, such as non-specific stimuli owing to hair removal, need for excessive dose of materials (e.g., allergens and chemicals) for sufficient skin application, and unavoidable use of certain mouse strains. To develop an experimental model to addresses the existing limitations, we noted some studies that induced AD using a relatively simple method, such as the application of an allergen on the ears of normal mice (Choi et al. 2011; Choi & Kim 2014). Taking a cue from those studies, we attempted to construct a murine experimental model for AM by combining their methods for AD development with the

conventional approach for asthma induction without the co-administration of any adjuvant at the sensitization stage, as our preliminary study and other research findings (Raemdonck et al. 2016) allowed us to anticipate that asthma was sufficiently induced without an adjuvant. As a result, our findings from the combination model indicated successful establishment of a practical model representing AM-mimicking conditions. We demonstrate that our murine experimental model for AM might contribute to improving previous AM models in terms of AD induction by minimizing skin irritation and simplifying allergen application.

Stepwise integrated analyses, including 2-DE, MS, functional annotation, and PPI, revealed that Hspa8 has potential as candidate biomarkers for AM. A number of biomarkers for allergic diseases have been studied using various analyses, such as omics technologies (Eguiluz-Gracia et al. 2018; Zissler et al. 2016). Although diverse cells and mediators in blood or sputum have been proposed as biomarkers for allergic diseases, AM biomarkers have been poorly investigated, except for several genetic factors. Filaggrin, a well-known predisposing factor for AM, when mutated remains significantly associated with AD and allergen sensitization and increased severity of asthma (Palmer et al. 2007; Thomsen 2015). The importance of filaggrin for AM was demonstrated in filaggrin-deficient mice that developed spontaneous dermatitis and pulmonary inflammation (Saunders et al. 2016). Several studies have suggested that polymorphisms in the genes encoding thymic stromal lymphopoietin and IL-33 are associated with the risk of AD and asthma (Harada et al. 2011; Margolis et al. 2014; Savenije et al. 2014; Shimizu et al. 2005). However, our exploration for candidate biomarkers in this study mainly focused on proteins measurable in biological fluids, which can be obtained more easily. By combining our results from the stepwise functional analyses, starting with exploring proteins differentially expressed in the BALF, we could have determined Hspa8 as a candidate biomarker. Hspa8, also termed heat shock cognate protein 70, belongs to the heat shock protein (HSP) 70 family and plays an important role in protein quality control, such as protein folding and antigen presentation by major histocompatibility complex class II molecules to T cells (Bonam et al. 2019). Hspa8 is also referred to as a major chaperone of the chaperone-mediated autophagy process, which is an intracellular degradation mechanism, and it acts as a key component binding to client substrates and delivering them to the lysosome membrane (Wang & Muller 2015). Although several studies have shown that exogenous Hspa8 could suppress lipopolysaccharide-induced inflammation in macrophages and attenuate dysfunction with anti-inflammatory responses in experimental septic

shock (Hsu et al. 2014; Sulistyowati et al. 2018), its function in allergic conditions is still unknown. Hspa8 was constitutively expressed and relatively less expressed during cellular stress, unlike Hsp70, which is otherwise known as a typical stress-inducible protein (Bonam et al. 2019). However, our findings indicated that the expression of Hspa8 might be increased in situations where chronic inflammation persists. Furthermore, the anti-inflammatory response mediated by exogenous Hspa8 is thought to be a key function that contributes to unveiling its role in the immune network and clarifying its association with allergic diseases.

There are several limitations in this study. First, it is controversial that several observations in the asthma-only induced group were less strong; this could be owing to the low allergen dose in this study compared to that used in a conventional murine model for asthma. The allergen was administered at a low dose in our model because we assumed that if asthma was strongly induced, it might mask the change of symptoms triggered by AM; further studies are warranted to alleviate this concern. Second, significant associations for Hspa8 were obtained only by statistical analysis, which requires validation by functional or pathophysiological studies. In other respects, it might also be important not to overlook the candidate proteins that are functionally close or more approachable experimentally, even though they showed relatively less significant associations. In this regards, further studies are underway to ascertain if the ferritin light chain, which showed only limited significance in our integrated analyses, might play a certain role in allergic response.

Conclusions

In conclusion, we established a murine model for AM that could minimize skin irritation and simplify the application of allergen during AD induction. Based on this improved AM model, we found that Hspa8 showed a significant association through stepwise functional analyses. Taken together, our findings provide novel evidence that Hspa8 has potential as a candidate biomarker for AM. Although several studies have refuted the concept of AM and asserted that the prevalence of AM has been overemphasized, it should be recognized that research on AM can provide a new perspective for early prevention, diagnosis, and treatment of allergic diseases (Yang et al. 2020). We expect that our findings will provide better knowledge of experimental models for AM and novel targets for new treatment strategies for allergic diseases.

Acknowledgements

This work was supported by research grants (2016-NI67002-00, 2017-NG67001-00, 2017-NG67001-01, 2017-NG67001-02, and 2020-NG-009-00, 2020-NG-009-01) from the Korea Disease Control and Prevention Agency.

References

Aw M, Penn J, Gauvreau GM, Lima H, and Sehmi R. 2020. Atopic March: Collegium Internationale Allergologicum Update 2020. Int Arch Allergy Immunol 181:1-10. 10.1159/000502958

Bantz SK, Zhu Z, and Zheng T. 2014. The Atopic March: Progression from Atopic Dermatitis to Allergic Rhinitis and Asthma. J Clin Cell Immunol 5. 10.4172/2155-9899.1000202

Bonam SR, Ruff M, and Muller S. 2019. HSPA8/HSC70 in Immune Disorders: A Molecular Rheostat that Adjusts Chaperone-Mediated Autophagy Substrates. Cells 8. 10.3390/cells8080849

Busse WW. 2018. The atopic march: Fact or folklore? Ann Allergy Asthma Immunol 120:116-118. 10.1016/j.anai.2017.10.029

Choi EJ, Lee S, Kim HH, Singh TS, Choi JK, Choi HG, Suh WM, Lee SH, and Kim SH. 2011. Suppression of dust mite extract and 2,4-dinitrochlorobenzene-induced atopic dermatitis by the water extract of Lindera obtusiloba. J Ethnopharmacol 137:802-807. 10.1016/j.jep.2011.06.043

Choi JK, and Kim SH. 2014. Inhibitory effect of galangin on atopic dermatitis-like skin lesions. Food Chem Toxicol 68:135-141. 10.1016/j.fct.2014.03.021

Cohn L, Elias JA, and Chupp GL. 2004. Asthma: mechanisms of disease persistence and progression. Annu Rev Immunol 22:789-815. 10.1146/annurev.immunol.22.012703.104716

del Giudice MM, Rocco A, and Capristo C. 2006. Probiotics in the atopic march: highlights and new insights. Dig Liver Dis 38 Suppl 2:S288-290. 10.1016/s1590-8658(07)60012-7

Eder W, Ege MJ, and von Mutius E. 2006. The asthma epidemic. N Engl J Med 355:2226-2235. 10.1056/NEJMra054308

366 Eguiluz-Gracia I, Tay TR, Hew M, Escribese MM, Barber D, O'Hehir RE, and Torres MJ. 2018.
367 Recent developments and highlights in biomarkers in allergic diseases and asthma. Allergy
368 73:2290-2305. 10.1111/all.13628
369 Gustafsson D, Sjöberg O, and Foucard T. 2000. Development of allergies and asthma in infants
370 and young children with atopic dermatitis--a prospective follow-up to 7 years of age. Allergy
371 55:240-245. 10.1034/j.1398-9995.2000.00391.x
372 Han H, Roan F, and Ziegler SF. 2017. The atopic march: current insights into skin barrier
373 dysfunction and epithelial cell-derived cytokines. Immunol Rev 278:116-130.
374 10.1111/imr.12546
375 Harada M, Hirota T, Jodo AI, Hitomi Y, Sakashita M, Tsunoda T, Miyagawa T, Doi S, Kameda
376 M, Fujita K, Miyatake A, Enomoto T, Noguchi E, Masuko H, Sakamoto T, Hizawa N, Suzuki
377 Y, Yoshihara S, Adachi M, Ebisawa M, Saito H, Matsumoto K, Nakajima T, Mathias RA,
378 Rafaels N, Barnes KC, Himes BE, Duan QL, Tantisira KG, Weiss ST, Nakamura Y, Ziegler
379 SF, and Tamari M. 2011. Thymic stromal lymphopoietin gene promoter polymorphisms are
380 associated with susceptibility to bronchial asthma. Am J Respir Cell Mol Biol 44:787-793.
381 10.1165/rcmb.2009-0418OC
382 Hill DA, and Spergel JM. 2018. The atopic march: Critical evidence and clinical relevance. Ann
383 Allergy Asthma Immunol 120:131-137. 10.1016/j.anai.2017.10.037
384 Hogan MB, Peele K, and Wilson NW. 2012. Skin barrier function and its importance at the start
385 of the atopic march. J Allergy (Cairo) 2012:901940. 10.1155/2012/901940
386 Hsu JH, Yang RC, Lin SJ, Liou SF, Dai ZK, Yeh JL, and Wu JR. 2014. Exogenous heat shock
387 cognate protein 70 pretreatment attenuates cardiac and hepatic dysfunction with associated
388 anti-inflammatory responses in experimental septic shock. Shock 42:540-547.
389 10.1097/shk.0000000000000254
390 Huang da W, Sherman BT, and Lempicki RA. 2009. Systematic and integrative analysis of large
391 gene lists using DAVID bioinformatics resources. Nat Protoc 4:44-57.
392 10.1038/nprot.2008.211
393 Huang da W, Sherman BT, Stephens R, Baseler MW, Lane HC, and Lempicki RA. 2008.
394 DAVID gene ID conversion tool. Bioinformation 2:428-430. 10.6026/97320630002428
395 Justice MJ, and Dhillon P. 2016. Using the mouse to model human disease: increasing validity
396 and reproducibility. Dis Model Mech 9:101-103. 10.1242/dmm.024547

Kim HJ, Kim YJ, Lee SH, Yu J, Jeong SK, and Hong SJ. 2014. Effects of Lactobacillus rhamnosus on allergic march model by suppressing Th2, Th17, and TSLP responses via CD4(+)CD25(+)Foxp3(+) Tregs. Clin Immunol 153:178-186. 10.1016/j.clim.2014.04.008

Kim MH, Choi YY, Yang G, Cho IH, Nam D, and Yang WM. 2013. Indirubin, a purple 3,2-bisindole, inhibited allergic contact dermatitis via regulating T helper (Th)-mediated immune system in DNCB-induced model. J Ethnopharmacol 145:214-219. 10.1016/j.jep.2012.10.055

Lee HJ, Lee NR, Jung M, Kim DH, and Choi EH. 2015. Atopic March from Atopic Dermatitis to Asthma-Like Lesions in NC/Nga Mice Is Accelerated or Aggravated by Neutralization of Stratum Corneum but Partially Inhibited by Acidification. J Invest Dermatol 135:3025-3033. 10.1038/jid.2015.333

Lee HJ, Yoon NY, Lee NR, Jung M, Kim DH, and Choi EH. 2014. Topical acidic cream prevents the development of atopic dermatitis- and asthma-like lesions in murine model. Exp Dermatol 23:736-741. 10.1111/exd.12525

Margolis DJ, Kim B, Apter AJ, Gupta J, Hoffstad O, Papadopoulos M, and Mitra N. 2014. Thymic stromal lymphopoietin variation, filaggrin loss of function, and the persistence of atopic dermatitis. JAMA Dermatol 150:254-259. 10.1001/jamadermatol.2013.7954

Odhiambo JA, Williams HC, Clayton TO, Robertson CF, and Asher MI. 2009. Global variations in prevalence of eczema symptoms in children from ISAAC Phase Three. J Allergy Clin Immunol 124:1251-1258.e1223. 10.1016/j.jaci.2009.10.009

Palmer CN, Ismail T, Lee SP, Terron-Kwiatkowski A, Zhao Y, Liao H, Smith FJ, McLean WH, and Mukhopadhyay S. 2007. Filaggrin null mutations are associated with increased asthma severity in children and young adults. J Allergy Clin Immunol 120:64-68. 10.1016/j.jaci.2007.04.001

Platts-Mills TA. 2015. The allergy epidemics: 1870-2010. J Allergy Clin Immunol 136:3-13. 10.1016/j.jaci.2015.03.048

Raemdonck K, Baker K, Dale N, Dubuis E, Shala F, Belvisi MG, and Birrell MA. 2016. $CD4^+$ and $CD8^+$ T cells play a central role in a HDM driven model of allergic asthma. Respir Res 17:45. 10.1186/s12931-016-0359-y

Saunders SP, Moran T, Floudas A, Wurlod F, Kaszlikowska A, Salimi M, Quinn EM, Oliphant CJ, Núñez G, McManus R, Hams E, Irvine AD, McKenzie AN, Ogg GS, and Fallon PG. 2016. Spontaneous atopic dermatitis is mediated by innate immunity, with the secondary lung

inflammation of the atopic march requiring adaptive immunity. J Allergy Clin Immunol 137:482-491. 10.1016/j.jaci.2015.06.045

Savenije OE, Mahachie John JM, Granell R, Kerkhof M, Dijk FN, de Jongste JC, Smit HA, Brunekreef B, Postma DS, Van Steen K, Henderson J, and Koppelman GH. 2014. Association of IL33-IL-1 receptor-like 1 (IL1RL1) pathway polymorphisms with wheezing phenotypes and asthma in childhood. J Allergy Clin Immunol 134:170-177. 10.1016/j.jaci.2013.12.1080

Schneider L, Hanifin J, Boguniewicz M, Eichenfield LF, Spergel JM, Dakovic R, and Paller AS. 2016. Study of the Atopic March: Development of Atopic Comorbidities. Pediatr Dermatol 33:388-398. 10.1111/pde.12867

Shannon P, Markiel A, Ozier O, Baliga NS, Wang JT, Ramage D, Amin N, Schwikowski B, and Ideker T. 2003. Cytoscape: a software environment for integrated models of biomolecular interaction networks. Genome Res 13:2498-2504. 10.1101/gr.1239303

Shimizu M, Matsuda A, Yanagisawa K, Hirota T, Akahoshi M, Inomata N, Ebe K, Tanaka K, Sugiura H, Nakashima K, Tamari M, Takahashi N, Obara K, Enomoto T, Okayama Y, Gao PS, Huang SK, Tominaga S, Ikezawa Z, and Shirakawa T. 2005. Functional SNPs in the distal promoter of the ST2 gene are associated with atopic dermatitis. Hum Mol Genet 14:2919-2927. 10.1093/hmg/ddi323

Sulistyowati E, Lee MY, Wu LC, Hsu JH, Dai ZK, Wu BN, Lin MC, and Yeh JL. 2018. Exogenous Heat Shock Cognate Protein 70 Suppresses LPS-Induced Inflammation by Down-Regulating NF-κB through MAPK and MMP-2/-9 Pathways in Macrophages. Molecules 23. 10.3390/molecules23092124

Szklarczyk D, Gable AL, Lyon D, Junge A, Wyder S, Huerta-Cepas J, Simonovic M, Doncheva NT, Morris JH, Bork P, Jensen LJ, and Mering CV. 2019. STRING v11: protein-protein association networks with increased coverage, supporting functional discovery in genome-wide experimental datasets. Nucleic Acids Res 47:D607-d613. 10.1093/nar/gky1131

Thomsen SF. 2015. Epidemiology and natural history of atopic diseases. Eur Clin Respir J 2. 10.3402/ecrj.v2.24642

Tran MM, Lefebvre DL, Dharma C, Dai D, Lou WYW, Subbarao P, Becker AB, Mandhane PJ, Turvey SE, and Sears MR. 2018. Predicting the atopic march: Results from the Canadian Healthy Infant Longitudinal Development Study. J Allergy Clin Immunol 141:601-607.e608. 10.1016/j.jaci.2017.08.024

Wang F, and Muller S. 2015. Manipulating autophagic processes in autoimmune diseases: a special focus on modulating chaperone-mediated autophagy, an emerging therapeutic target. Front Immunol 6:252. 10.3389/fimmu.2015.00252

Yang L, Fu J, and Zhou Y. 2020. Research Progress in Atopic March. Front Immunol 11:1907. 10.3389/fimmu.2020.01907

Zissler UM, Esser-von Bieren J, Jakwerth CA, Chaker AM, and Schmidt-Weber CB. 2016. Current and future biomarkers in allergic asthma. Allergy 71:475-494. 10.1111/all.12828

Figure legends

Figure 1. Experimental protocol for the allergic march model in mice. The induction of atopic dermatitis was achieved by the topical application of 1% 2,4-dinitrochlorobenzene (20 μL), followed by 75 μg of *Dermatophagoides pteronyssinus* (Dp) on the ear skin for 5 weeks. To develop a barrier disruption, 20 μL of 4% sodium dodecyl sulfate was applied 4 h before Dp application. Allergic asthma was subsequently induced by two intraperitoneal Dp sensitization and intranasal challenges for four consecutive days. After the last intranasal administration, airway hyperresponsiveness was measured, and then, bronchoalveolar lavage fluid and lung tissue were obtained for further analysis. Mice were randomly divided into four groups (n = 5 per group). NC, normal control; AD, atopic dermatitis; AS, asthma; AM, atopic march.

Figure 2. Induction of atopic dermatitis (AD). (A) Typical photographs of mouse ears from each group. AD-like lesions were observed at various stages as indicated after starting AD induction by repeatedly applying 2,4-dinitrochlorobenzene and Dp extract for 5 weeks. (B) Total immunoglobulin E (IgE) levels in plasma. Blood samples were collected from Dp-applied and normal control mice at day 8 and 22 during the AD induction. The levels of total IgE in plasma was significantly higher in the Dp-applied group than in the normal control group. All data are representative of three independent experiments with similar results. Data are presented as the mean ± standard error of the mean (SEM) (n = 5 per group). $^{*}p < 0.05$ and $^{***}p < 0.001$ versus the normal control group

Figure 3. Analysis of airway hyperresponsiveness (AHR) and airway inflammation in the mouse model of Dp extract-induced atopic march (AM). (A) Aggravated AHR in response to methacholine. After 24 h of the final intranasal challenge, mice were stimulated with increasing doses of aerosolized methacholine (12.5, 25, and 50 mg/mL). Airway resistance and dynamic compliance were significantly aggravated owing to the development of AM. (B) The number of various immune cells in the bronchoalveolar lavage fluid (BALF). Increased number of cells indicated the induction of airway inflammation with the development of AM. The number of eosinophils was higher in the BALF obtained from the AM-induced group than in that from the BALF from the AD or asthma-only induced groups. (C) Representative hematoxylin and eosin-stained sections for lung histology in each experimental group (magnification, 200X; scale bar = 50 μm). Cell infiltration in the lung was worse in the AM-induced group than in the other groups. All data are representative of three independent experiments with similar results. Data are presented as the mean ± standard error of the mean (SEM) (n = 5 per group). Values represent mean ± SEM. $^{\#}p < 0.05$ versus AM group. $^{**}p < 0.01$, $^{***}p < 0.001$ versus the normal control group.

Figure 4. Elevated level of immunoglobulin E (IgE) and cytokines caused by AM development. The plasma levels of total IgE (A) and *Dermatophagoides pteronyssinus*-specific IgE (B) and the levels of interleukin (IL)-4 (C), IL-5 (D), IL-13 (E), and interferon (IFN)-γ (F) in bronchoalveolar lavage fluid were measured by enzyme-linked immunosorbent assay. These data showed a significant increase in allergic responses with the development of AM compared with the other groups. All data are representative of three independent experiments with similar results. Data are presented as the mean ± standard error of the mean (SEM) (n = 5 per group). Values represent mean ± SEM. $^{\#}p < 0.05$, $^{\#\#}p < 0.01$, and $^{\#\#\#}p < 0.001$ versus AM-induced mice. $^{*}p < 0.05$, $^{**}p < 0.01$, and $^{***}p < 0.001$ versus the normal control group.

Figure 5. Protein-protein interaction (PPI) network and identification of heat shock protein 8 as a hub protein. PPI analysis of differentially expressed proteins in the Atopic march-induced and normal control groups. The yellow node represents hub proteins (degree > 10 as cut-off criterion), and the edge represents the interaction relationship among the proteins.

Figure 1

Experimental protocol for the allergic march model in mice

The induction of atopic dermatitis was achieved by the topical application of 1% 2,4-dinitrochlorobenzene (20 µL), followed by 75 µg of Dermatophagoides pteronyssinus (Dp) on the ear skin for 5 weeks. To develop a barrier disruption, 20 µL of 4% sodium dodecyl sulfate was applied 4 h before Dp application. Allergic asthma was subsequently induced by two intraperitoneal Dp sensitization and intranasal challenges for four consecutive days. After the last intranasal administration, airway hyperresponsiveness was measured, and then, bronchoalveolar lavage fluid and lung tissue were obtained for further analysis. Mice were randomly divided into four groups (n = 5 per group). NC, normal control; AD, atopic dermatitis; AS, asthma; AM, atopic march.

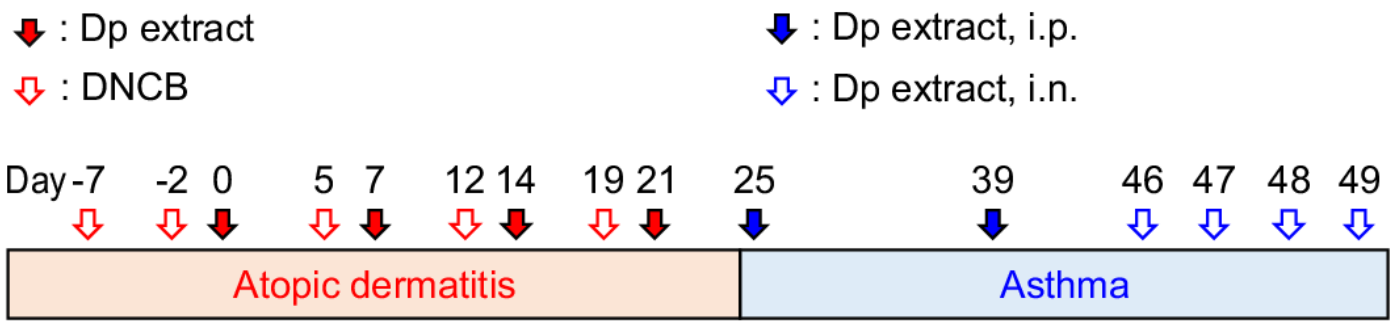

Figure 2

Induction of atopic dermatitis (AD)

(A) Typical photographs of mouse ears from each group. AD-like lesions were observed at various stages as indicated after starting AD induction by repeatedly applying 2,4-dinitrochlorobenzene and Dp extract for 5 weeks. (B) Total immunoglobulin E (IgE) levels in plasma. Blood samples were collected from Dp-applied and normal control mice at day 8 and 22 during the AD induction. The levels of total IgE in plasma was significantly higher in the Dp-applied group than in the normal control group. All data are representative of three independent experiments with similar results. Data are presented as the mean ± standard error of the mean (SEM) (n = 5 per group).*p < 0.05 and ***p < 0.001 versus the normal control group.

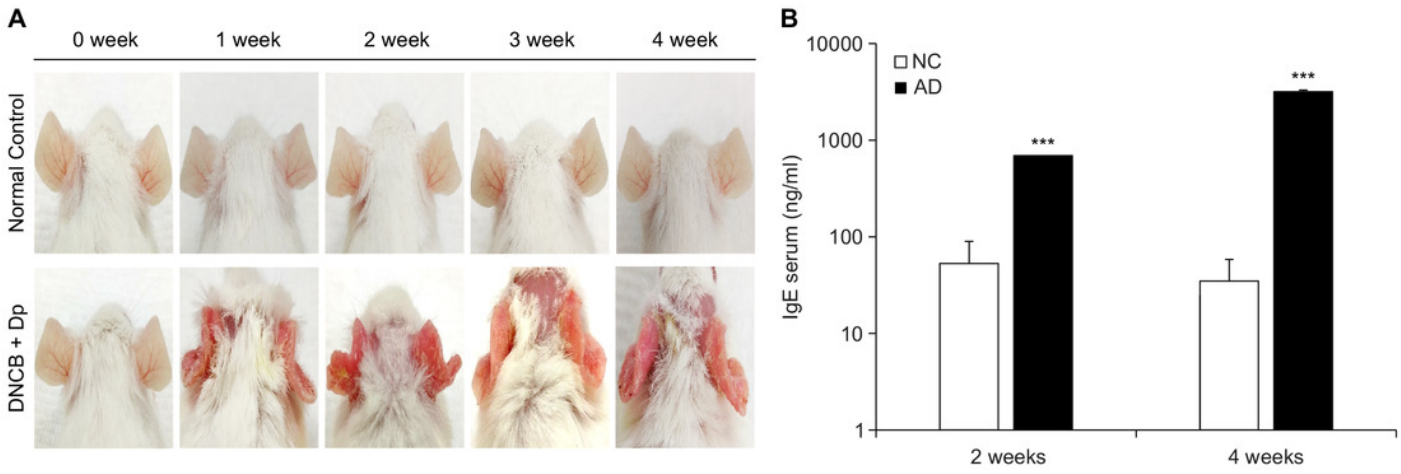

Figure 3

Analysis of airway hyperresponsiveness (AHR) and airway inflammation in the mouse model of Dp extract-induced atopic march (AM)

(A) Aggravated AHR in response to methacholine. After 24 h of the final intranasal challenge, mice were stimulated with increasing doses of aerosolized methacholine (12.5, 25, and 50 mg/mL). Airway resistance and dynamic compliance were significantly aggravated owing to the development of AM. (B) The number of various immune cells in the bronchoalveolar lavage fluid (BALF). Increased number of cells indicated the induction of airway inflammation with the development of AM. The number of eosinophils was higher in the BALF obtained from the AM-induced group than in that from the BALF from the AD or asthma-only induced groups. (C) Representative hematoxylin and eosin-stained sections for lung histology in each experimental group (magnification, 200X; scale bar = 50 μm). Cell infiltration in the lung was worse in the AM-induced group than in the other groups. All data are representative of three independent experiments with similar results. Data are presented as the mean ± standard error of the mean (SEM) (n = 5 per group). Values represent mean ± SEM. #$p < 0.05$ versus AM group. **$p < 0.01$, ***$p < 0.001$ versus the normal control group.

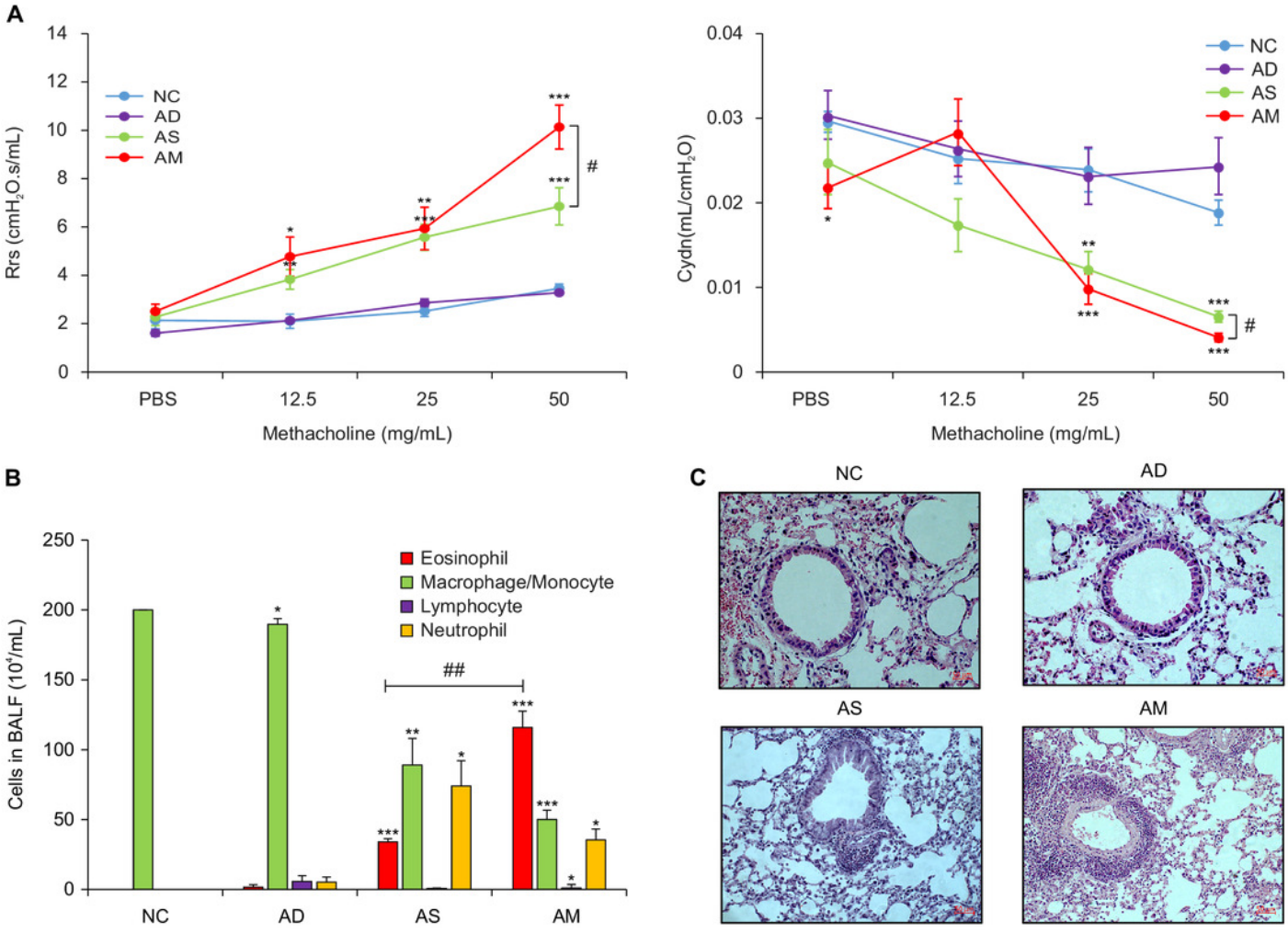
A
Rrs (cmH2O.s/mL)
NC
AD
AS
AM
PBS
12.5
25
50
Methacholine (mg/mL)
Cydn(mL/cmH2O)
B
Cells in BALF (10⁴/mL)
Eosinophil
Macrophage/Monocyte
Lymphocyte
Neutrophil
C

Figure 4

Elevated level of immunoglobulin E (IgE) and cytokines caused by AM development

The plasma levels of total IgE (A) and Dermatophagoides pteronyssinus-specific IgE (B) and the levels of interleukin (IL)-4 (C), IL-5 (D), IL-13 (E), and interferon (IFN)-γ (F) in bronchoalveolar lavage fluid were measured by enzyme-linked immunosorbent assay. These data showed a significant increase in allergic responses with the development of AM compared with the other groups. All data are representative of three independent experiments with similar results. Data are presented as the mean ± standard error of the mean (SEM) (n = 5 per group). Values represent mean ± SEM. #$p < 0.05$, ##$p < 0.01$, and ###$p < 0.001$ versus AM-induced mice. *$p < 0.05$, **$p < 0.01$, and ***$p < 0.001$ versus the normal control group.

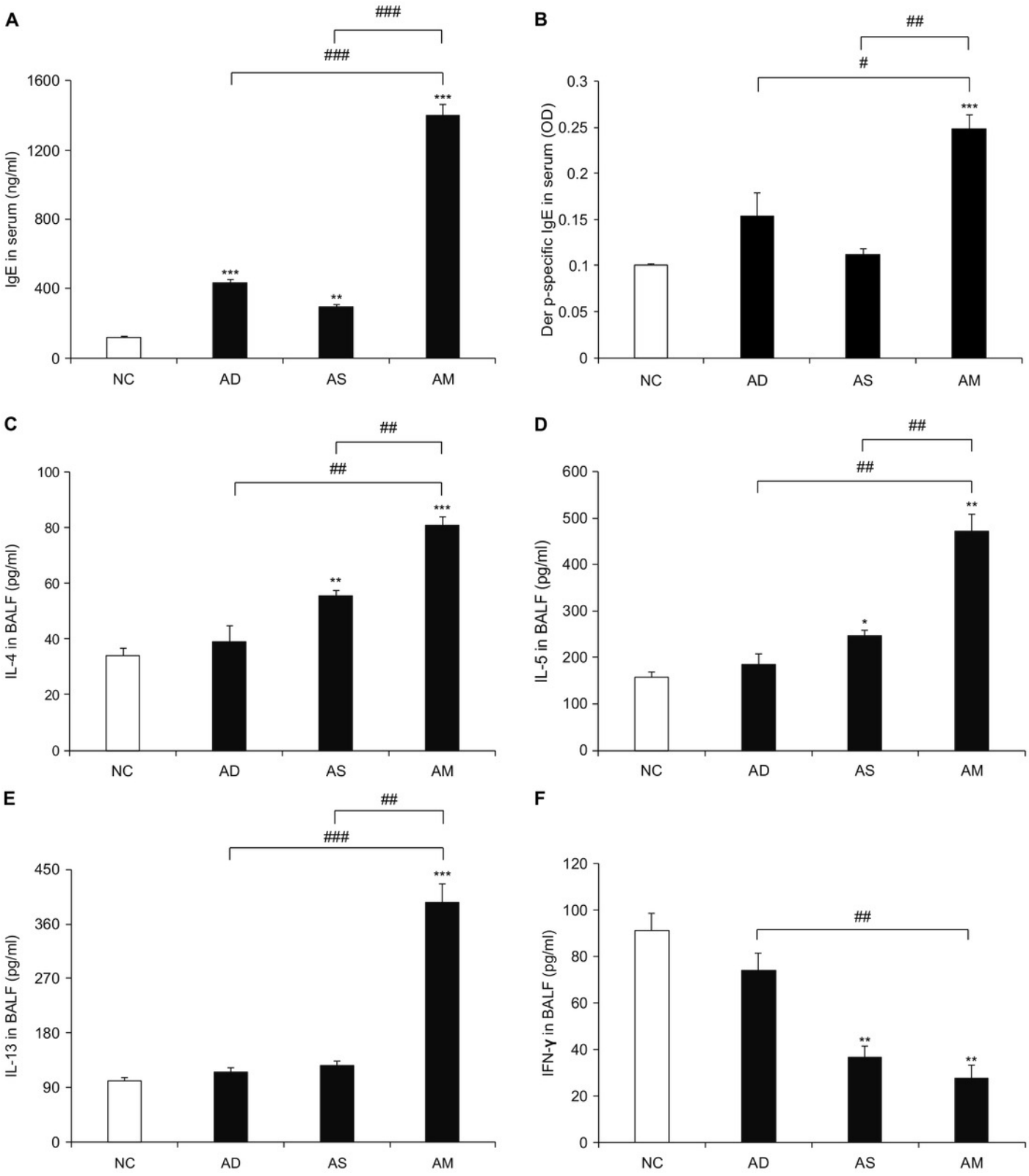
A
IgE in serum (ng/ml)
1600
1200
800
400
0
###
###
***
***
**
NC
AD
AS
AM
B
Der p-specific IgE in serum (OD)
0.3
0.25
0.2
0.15
0.1
0.05
0
##
#
***
NC
AD
AS
AM
C
IL-4 in BALF (pg/ml)
100
80
60
40
20
0
##
##
***
**
NC
AD
AS
AM
D
IL-5 in BALF (pg/ml)
600
500
400
300
200
100
0
##
##
**
*
NC
AD
AS
AM
E
IL-13 in BALF (pg/ml)
450
360
270
180
90
0
##
###
***
NC
AD
AS
AM
F
IFN-γ in BALF (pg/ml)
120
100
80
60
40
20
0
##
**
**
NC
AD
AS
AM

Figure 5

Protein-protein interaction (PPI) network and identification of heat shock protein 8 as a hub protein

PPI analysis of the differentially expressed proteins in the atopic march-induced and normal control groups. The yellow node represents hub proteins (degree > 10 as cut-off criterion) and the edge represents the interaction relationship among the proteins.

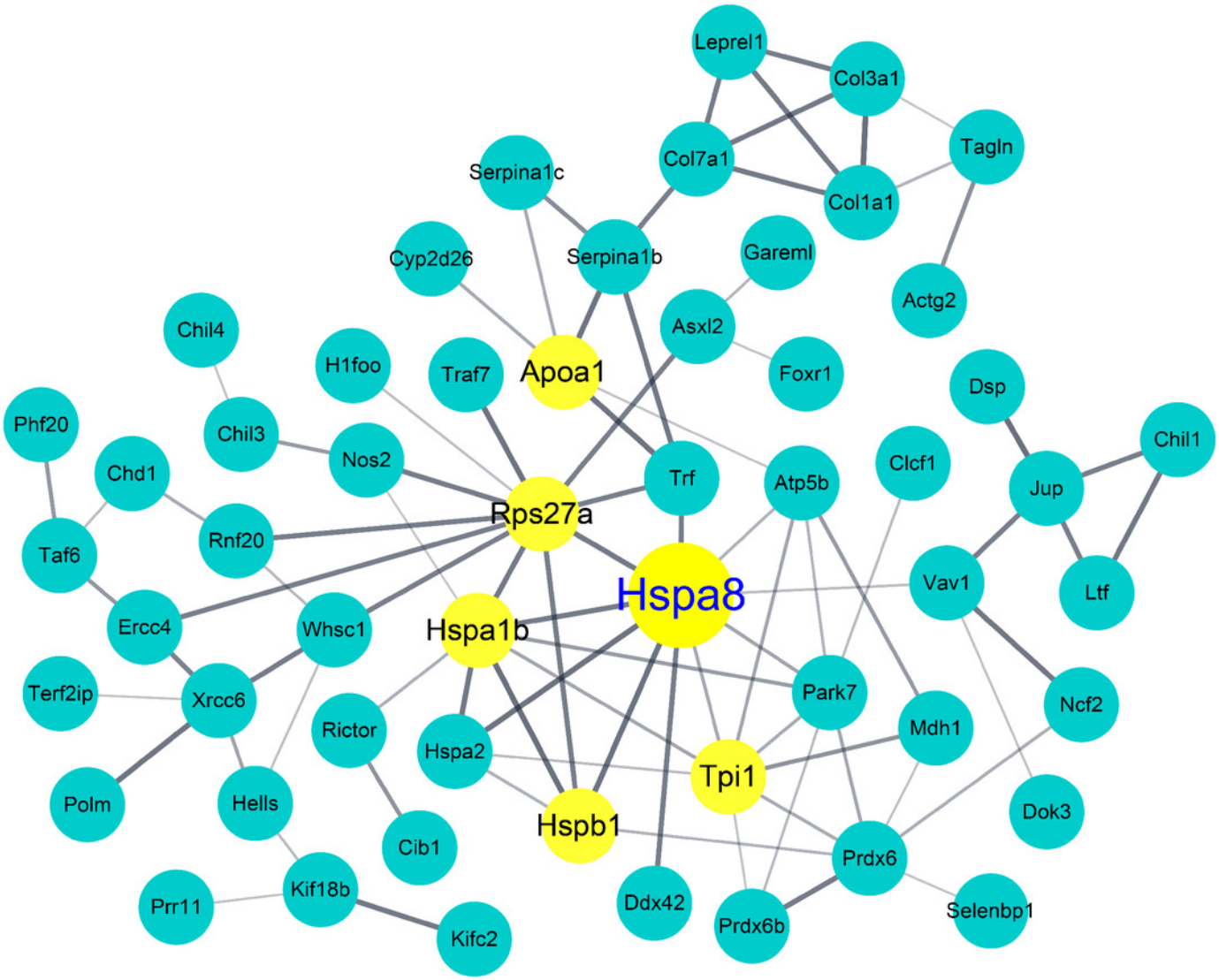

Table 1(on next page)

Top 10 GO enrichment terms for differentially expressed proteins between the AM-induced group and the normal control

Table 1. Top 10 GO enrichment terms for differentially expressed proteins between the AM-induced group and the normal control

Category	Description	Count	*P* value	Top 3 Proteins (total number of proteins)
CC	GO:0005615 ~extracellular space	36	9.58E-09	**Heat shock protein 8** Lactotransferrin Collagen, type III, α1 (140)
BP	GO:0034097 ~response to cytokine	9	3.23E-07	Collagen, type III, α1 Serpina1b protein Serpina3f protein (34)
CC	GO:0072562 ~blood microparticle	10	1.36E-06	**Heat shock protein 8** Serotransferrin α-fetoprotein (62)
CC	GO:0070062 ~extracellular exosome	45	2.11E-06	**Heat shock protein 8** Lactotransferrin Kalirin (160)
BP	GO:0043434 ~response to peptide hormone	8	2.21E-06	Serpina1b protein Serpina3f protein serine peptidase inhibitor (34)
CC	GO:0031012 ~extracellular matrix	12	2.82E-05	**Heat shock protein 8** Collagen, type III, α1 Peroxidasin homolog (55)
MF	GO:0004867 ~serine-type endopeptidase inhibitor activity	8	8.21E-05	Serpina1b protein Serpina3f protein serine peptidase inhibitor (17)
CC	GO:0005829 ~cytosol	30	2.12E-04	**Heat shock protein 8** Kinesin 2, isoform Peroxiredoxin-6 (139)
CC	GO:0005737 ~cytoplasm	76	2.92E-04	**Heat shock protein 8** Kinesin 2, isoform Lactotransferrin (265)
BP	GO:0010466 ~negative regulation of peptidase activity	7	4.03E-04	Serpina1b protein Serpina3f protein serine peptidase inhibitor (16)

* BP: Biological Process; CC: Cell Component; MF: Molecular Function.

Table 2(on next page)

Top 10 proteins according to degree, betweenness centrality, and closeness centrality as scored via PPI analysis

Table 2. Top 10 proteins according to degree, betweenness centrality, and closeness centrality as scored via PPI analysis

Proteins	Degree	Proteins	Betweenness centrality	Proteins	Closeness centrality
Hspa8	16	Rps27a	0.260756	**Hspa8**	0.470899
Hspa1b	14	**Hspa8**	0.208497	Hspa1b	0.451777
Rps27a	14	Hspa1b	0.13845	Hspb1	0.438424
Apoa1	11	Hspb1	0.079339	Rps27a	0.410138
Hspb1	11	Klc1	0.07388	Trf	0.402715
Tpi1	11	Vav1	0.069638	Tpi1	0.400901
Trf	10	Xrcc6	0.068084	Htt	0.39207
Serpina3n	10	Eif3c	0.067765	Atp5b	0.37395
Serpina3f	10	Htt	0.061455	Anxa5	0.369295
Serpina1d	10	Col1a1	0.055232	Apoa1	0.366255